NASA TN D-755

TECHNICAL NOTE

D-755

THE STIFFNESS PROPERTIES OF STRESSED FABRICS AS OBTAINED FROM MODEL TESTS

By George W. Zender and Jerry W. Deaton

Langley Research Center
Langley Field, Va.

NATIONAL AERONAUTICS AND SPACE ADMINISTRATION

WASHINGTON

August 1961

NATIONAL AERONAUTICS AND SPACE ADMINISTRATION

TECHNICAL NOTE D-755

THE STIFFNESS PROPERTIES OF STRESSED FABRICS AS OBTAINED FROM MODEL TESTS

By George W. Zender and Jerry W. Deaton

SUMMARY

The stiffness properties of a nylon-neoprene fabric material subjected to uniaxial, biaxial, or shear stresses as obtained from tests of simple models are presented. The stiffness properties are applicable to problems involving applied loads after the fabric is in an initial state of biaxial tension such as occurs upon inflation. The results demonstrate the inadequacy of uniaxial tests in obtaining the stiffness properties to be used in the design and analysis of inflatable fabric structures. In order to obtain proper stiffness values for use in the design and analysis of stressed fabric structures, tests of simple models of the type presented herein, subjected to stress conditions similar to those anticipated in the full-scale design, are recommended.

INTRODUCTION

Expandible structures have recently received considerable attention in the design of space vehicles, principally because of packaging requirements and the low loading intensities associated with space flight. Such structures have utilized many materials such as films and fabrics expanded by foams or gases. A particular fabric construction which has received attention is known as Airmat and was developed by the Goodyear Aircraft Corporation. Contained herein are the results of tests performed to determine the material properties of a particular nylon-neoprene Airmat fabric (manufacturer's designation XA27A209) which has been used at the Langley Research Center in structural studies of inflatable structures. (See ref. 1.)

TEST SPECIMENS AND METHOD OF TESTING

The Airmat fabric used for the present investigation consists of two material surfaces tied together with "drop" yarns that provide a

1-inch space between surfaces, when inflated. (See fig. 1(a).) Each surface consists of an inner ply of nylon Airmat weave, and a cover ply of plain weave coated with neoprene to contain the inflation gas. Other details of the fabric are given in table I. Both the inner and cover ply shown in figure 1(a) contain one set of yarns with considerable crimp while the other set of yarns is more nearly straight. (See fig. 1(b).) The inner and cover plys are oriented at 90° to each other so that the crimped yarns of one ply are alined with the more nearly straight yarns of the remaining ply. For purposes of specifying orientation of the material, the directions of the yarns of the heavier inner ply (fig. 1(b)) are employed, that is, the direction of the warp yarns of the inner ply is termed the warp direction of the material, whereas the direction transverse to the warp direction (that of the more nearly straight yarns of the inner ply) is termed the fill direction.

Three types of specimen were tested. One type was a plain strip of the fabric; a second was constructed as a beam and the third, as a cylinder. General details of each type are shown in figure 2. The cylinders were made of one surface of the Airmat material obtained by severing the drop yarns so that approximately 1/2 inch of length of the drop yarns remained with the surface material. The surface material was then fabricated into cylindrical form by splicing the two opposite sides of the surface together as shown in figure 2(c). The strip and beam specimens contained an extra-heavy coating of neoprene as evidenced by the comparisons of the weight per unit surface area shown in figure 2. The weights per unit surface area are based on the total surface area excluding the ends of the specimens. Two specimens of each type were tested, one with the warp yarns and one with the fill yarns oriented in the longitudinal direction of the specimen.

The strip specimens were subjected to tensile loads with deadweights (inner surfaces adjacent during test rather than with extended drop yarns indicated in fig. 2). The beams were inflated with air and subjected to end bending moments or longitudinal tensile loads as shown in figures 3 and 4. The cylinders were pressurized with air and subjected to torsion as shown in figure 5.

Strains on the strip and beam specimens were measured with Tuckerman optical strain gages of 1- or 2-inch gage length. Longitudinal and transverse strains were obtained at the center of each cover surface. One of the characteristics of woven materials is that the strain under load is time-dependent. Figure 6 demonstrates the variation of strain with time for a strip of the material subjected to a constant uniaxial loading of 9 lb/in. in the warp direction. Also shown in this figure is the time dependency of the strain when the load is removed. It is apparent from the results of figure 6 that

careful timing is required to obtain useful strain data from test specimens.

For the strip and beam specimens, the strain measurements obtained at each load increment were read after sufficient time had elapsed (approximately 5 minutes) for the strain not to be changing rapidly with time. Loads were applied progressively without unloading until maximum load was reached.

The twist of the head at the loaded end of the cylinders was measured by using an indicating arm attached to the head and a protractor of 15-inch radius mounted to the supporting frame. In order to prevent large lateral displacements of the axis of the cylinders, the loading head contained a pin which extended through a loosely fitting hole in the supporting frame shown in figure 5. Twist measurements were obtained by using the same loading and timing procedure as described for the strips and beams. Pressures were measured with a standard pressure gage and all tests were performed at room temperature (approximately 80° F).

RESULTS

Strip Tests

Figure 7 shows the stress-strain characteristics of the fabric for uniaxial load in the warp or fill direction. The data shown by the square test-point symbols pertain to strips of the spliced fabric and are discussed in the subsequent section on beam specimens. The data shown by the solid curves faired through the circular symbols are the results obtained for increasing load on the strip specimens while the dashed curves through the circular symbols show the results for unloading. Also indicated in figure 7 is the value of Poisson's ratio, obtained from the ratio of the transverse strain to longitudinal strain at the various stress levels, for increasing load and for decreasing load. The uniaxial results shown in figure 7 indicate that for the stress levels included herein, the stress-strain relationship is essentially linear for increasing load or strain except for the time-dependency effects discussed previously.

Beams Subjected to Pressure and Bending Moments or Tensile Loads

Table II shows the sectional properties used in determining the load per inch of width of the beam covers. The sectional properties

were evaluated from the assumed cross section which closely approximated the actual cross section as indicated by the sketch accompanying table II. For the calculations the effective thickness of the skin in the splice region was increased over that in the unspliced region in direct proportion to the increased stiffness of the spliced region of the actual beams over that of the unspliced region as determined from uniaxial tension tests. The square test-point symbols on figure 7 show the results of uniaxial tension tests obtained from the spliced portion of the beams which were cut from the beams after the main program of tests were completed. The splice specimens were 2.36 inches in width by 12 inches in length and included the beam fabric, splice fabric, and the adhesive material. For the curves for increasing load (fig. 7), the extensional stiffness in the warp direction for the fabric-plus-splice strip is 1.24 times that for the fabric alone. In the fill direction, the same splice material contributes more substantially to the extensional stiffness (fill count is less than warp count) and thus the corresponding value is 1.46. Therefore, for the beams assumed in the calculations, the effective thickness of the edge region was taken as 1.24 times that of the remainder of the beam for the beam with the warp in the longitudinal direction, while the similar value for the beam with the fill in the longitudinal direction was 1.46.

Figure 8 shows a typical set of results for the beam specimens. The results shown are for the inflation pressure of 15 psig and bending or tension. The curves labeled "due to pressure" show the longitudinal and transverse strain obtained for values of the longitudinal load per inch of width N_w as the beam was inflated to 15 psig internal pressure. The pressure then was maintained constant and bending moment was introduced, and the resulting longitudinal strains are given by the open circular symbols (darkened symbols indicate transverse strains) for the "tension" cover of the beam and by the square symbols for the "compression" cover ("tension" and "compression" refer to the components of the strain due to bending).

The data shown by the triangular symbols in figure 8 were obtained from the same beam used in the bending tests at the same pressure, but the beam was subjected to direct tensile loads as shown in figure 4. The symbols show the average of the strains measured on opposite sides of the specimen. A comparison of the results obtained from the tensile tests with the tensile data from the bending tests, tends to lend confidence to the method of accounting for the splice material, since the stress distribution in the splices differs considerably for the two cases.

A significant observation apparent in the data shown in figure 8 is the essentially linear nature of the stress-strain relationship for the fabric due to applied moments when the fabric is in an initial state of tension due to internal pressure. Such near-linearity indicates the

possibility of defining meaningful elastic constants which would be useful in the analysis of the behavior of a fabric structure as a result of load application after the structure has been inflated. Data similar to that shown in figure 8 were obtained for other pressures, and the longitudinal stiffnesses were obtained from the slopes of the lines faired through the data for the longitudinal strains for the tension and compression sides of the beams after pressurization. The results are shown in figure 9 for values of the transverse stress due to pressure for the various pressures investigated. The average values of Poisson's ratio corresponding to the transverse stress are also shown in figure 9. As indicated in figure 7 and by the transverse and longitudinal strain data of figure 8, the value of Poisson's ratio varies somewhat with stress level. Consequently, the values shown in figure 9 are the average of the values obtained for increasing load increments at a given pressure.

Cylinders Subjected to Pressure and Torsion

Figure 10 shows the torque-twist results obtained with the cylinders for values of the longitudinal stress at the various pressure levels. For small values of twist, the shear stiffness is approximately 100 lb/in. for both cylinders at all values of the pressure stresses tested. (The shear stiffness was evaluated from elementary torsion theory with the effect of the splice material neglected.) The stiffness falls off as the torque or twist increases and, as indicated in the figure, the shear stiffness is then dependent upon the pressure stress and the stress ratio as evidenced by the difference in the results obtained for the two cylinders. There was no buckling evident on the cylinders for the range included in figure 10.

DISCUSSION

It is evident from figure 9 that the presence of rather small transverse stresses contributes significantly to the extensional stiffness of the Airmat material over that obtained for uniaxial stresses. At stresses above 2 lb/in. in the fill direction, the extensional stiffness in the warp direction is reasonably constant. Similarly, the stiffness in the fill direction does not change appreciably when the stress in the warp direction is above 1 lb/in. The compressive stiffness in the warp direction is considerably less than the extensional stiffness in the warp direction, whereas the compressive stiffness in the fill direction is approximately the same as the extensional stiffness in the fill direction. Such behavior appears reasonable since the fill yarns are more nearly straight than the warp yarns and, consequently, the fill yarns are in a more favorable position to support compressive loads.

The values of Poisson's ratio for the fabric as shown in figure 9 are, in general, smaller than the values usually encountered for isotropic materials. The results show that the transverse stress does not appreciably affect the value of Poisson's ratio. Indeed the values of Poisson's ratio obtained from the strip tests (zero transverse stress) are essentially in line with the average of results for biaxial stresses. A considerable difference is indicated (fig. 9(a)) between the values of Poisson's ratio (warp direction) for tension for the beam loaded in bending and those for the beam loaded in tension. This difference results from the difference in the transverse strains of the beam when loaded in bending or tension, which is demonstrated by the darkened circular and triangular symbols in figure 8(a); however, the reason for the difference in transverse strains is unknown.

Figure 10 shows that the shear stiffness is approximately 100 lb/in. for low values of torque or twist, (up to about 1 lb/in. shear flow). This value of shear stiffness is approximately one-tenth the extensional stiffness of the fabric in the warp direction. This factor demonstrates the low in-plane shear stiffness of the material as compared with isotropic materials where the shear stiffness is usually about four-tenths the extensional stiffness. On the other hand, the shear stiffness is an order of magnitude greater than that indicated by analysis of a trellis model (see ref. 2) where the shear stiffness is equal to the pressure stress. The heavy neoprene coating on the fabric along with friction between fibers is probably largely responsible for the much larger shear stiffness than is indicated by the trellis-model analysis, although the splice material also contributed to the stiffness of the cylinders.

While the use of beams in the present investigation was convenient because of the unique construction of Airmat fabric, the use of cylinders is more practical for coated fabric materials in general. Pressurized cylinders may be subjected to tensile or compressive loads to obtain the proper stiffnesses. For such cylinders, two diametrically opposite splices are recommended, rather than a single splice as shown herein, in order to avoid large bending distortions of the cylinder. Cylinders are also convenient for bending or torsion tests. On small cylinders, however, both curvature and splices cause considerable difficulty in obtaining useful transverse strain data for use in evaluating Poisson's ratio.

CONCLUDING REMARKS

The stiffness properties of a particular nylon-neoprene fabric material subjected to uniaxial, biaxial, or shear stresses have been

presented. The stiffness properties are applicable to problems involving applied loads after the fabric is in an initial state of biaxial tension such as occurs upon inflation. The results demonstrate the inadequacy of uniaxial tests in obtaining stiffness properties to be used for fabric materials subjected to biaxial stress conditions. In order to obtain proper stiffness values for use in the design and analysis of stressed fabric structures, tests of simple models of the type included herein, subjected to stress conditions similar to those anticipated in the full-scale design, are recommended.

Langley Research Center,
National Aeronautics and Space Administration,
Langley Field, Va., March 24, 1961.

REFERENCES

1. Leonard, R. W., McComb, H. G., Jr., Zender, G. W., and Stroud, W. J.: Analysis of Inflated Reentry and Space Structures. Proc. of Recovery of Space Vehicles Symposium, Los Angeles, Calif., Aug. 31 - Sept. 1, 1960. (Sponsored by Inst. Aero. Sci. and Air Res. Dev. Command.)

2. Topping, A. D.: An Introduction to Biaxial Stress Problems in Fabric Structures. Aerospace Engineering, vol. 20, no. 4, April 1961.

TABLE I.- DETAILS OF FABRIC MATERIAL[a]

Item	Inner ply[b]	Cover ply[c]
Yarn material	Nylon	Nylon
Weave	Airmat	Plain
Weight, oz/sq yd of surface area	4.33	2.05
Warp count, ends/in.	82	105
Fill count, ends/in.	47	96
Drop-yarn count, ends/sq in.	88	-----

[a]Goodyear Aircraft Corporation XA27A209.

[b]Goodyear Aircraft Corporation 6877.

[c]Goodyear Aircraft Corporation 3511N.

TABLE II.- SECTIONAL PROPERTIES OF BEAMS

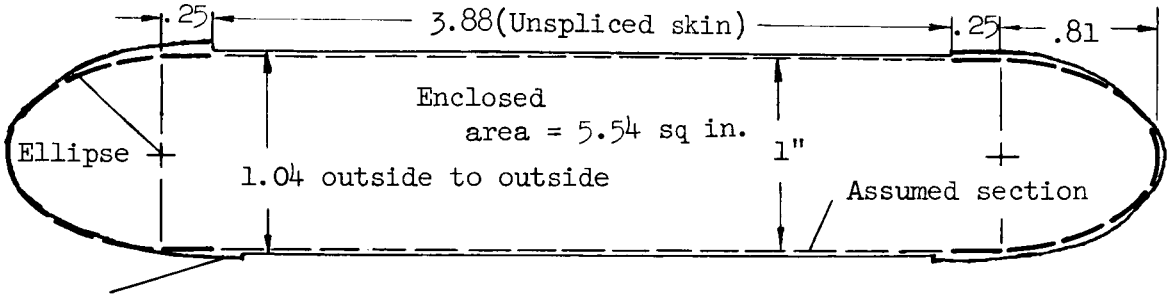

Trace of outer periphery of fill-longitudinal beam at 7 psig pressure

	Warp longitudinal	Fill longitudinal
$\frac{\text{Effective thickness at splice}}{\text{Unspliced thickness}}$, K (from fig. 7)	1.24	1.46
Effective periphery, in., for:		
Unspliced skin (2(3.88))	7.76	7.76
Spliced skin (2(0.5)K)	1.24	1.46
Spliced ellipse (4.1K)	5.08	5.98
Total	14.08	15.20
$\frac{\text{Effective moment of inertia}}{\text{Unspliced thickness}}$, $in.^3$, for:		
Unspliced skin $(2(3.88)(0.5)^2)$	1.94	1.94
Spliced skin $(2(0.5)(0.5)^2K)$	0.31	0.37
Spliced ellipse (0.5K)	0.62	0.73
Total	2.87	3.04

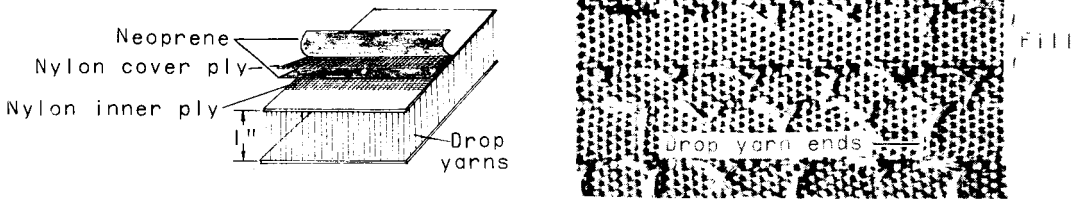

L-61-1072

(a) Airmat. (b) Photomicrograph of inner ply.

Figure 1.- Details of Airmat type of construction.

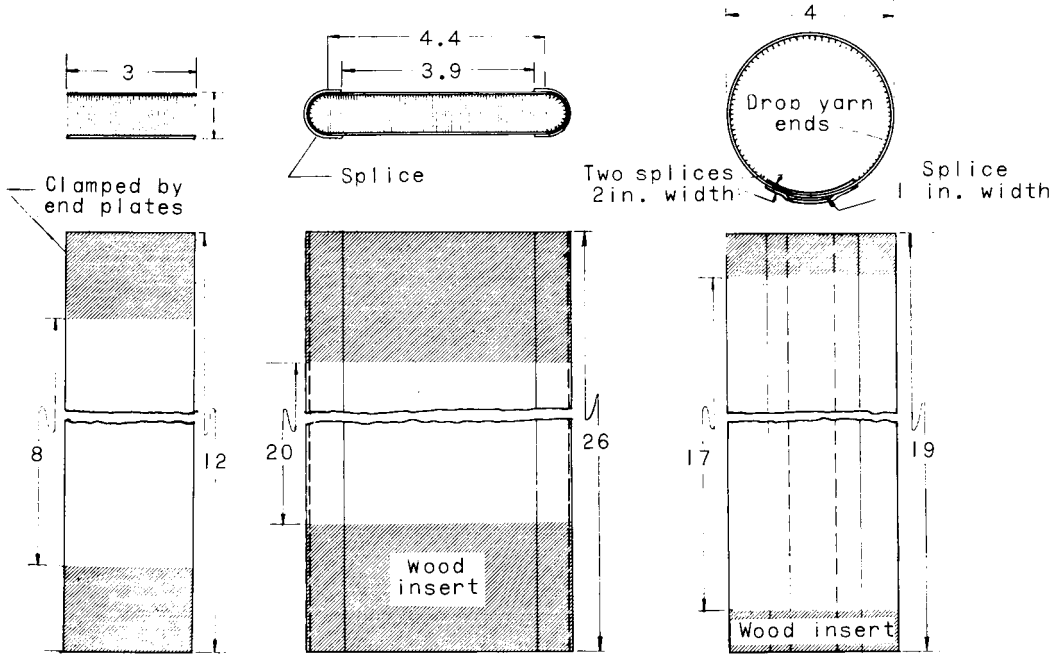

(a) Strip; $\frac{\text{Weight}}{\text{sq ft}} = 0.385$ lb.

(b) Beam; $\frac{\text{Weight}}{\text{sq ft}} = 0.420$ lb.

(c) Cylinder; $\frac{\text{Weight}}{\text{sq ft}} = 0.349$ lb (without splice, 0.288 lb).

Figure 2.- Details of test specimens. All dimensions are in inches.

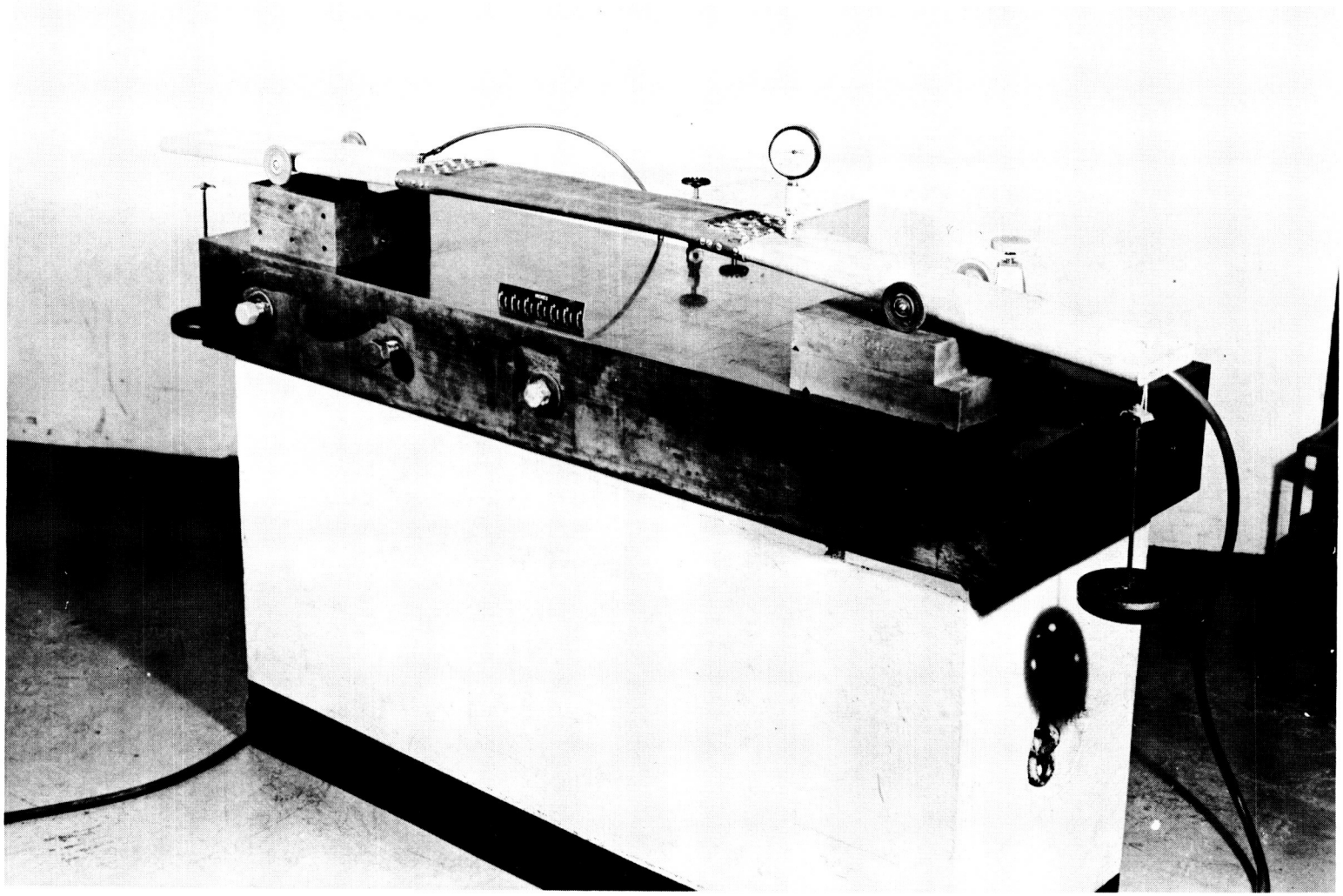

Figure 3.- Beam bending test setup. L-60-2871

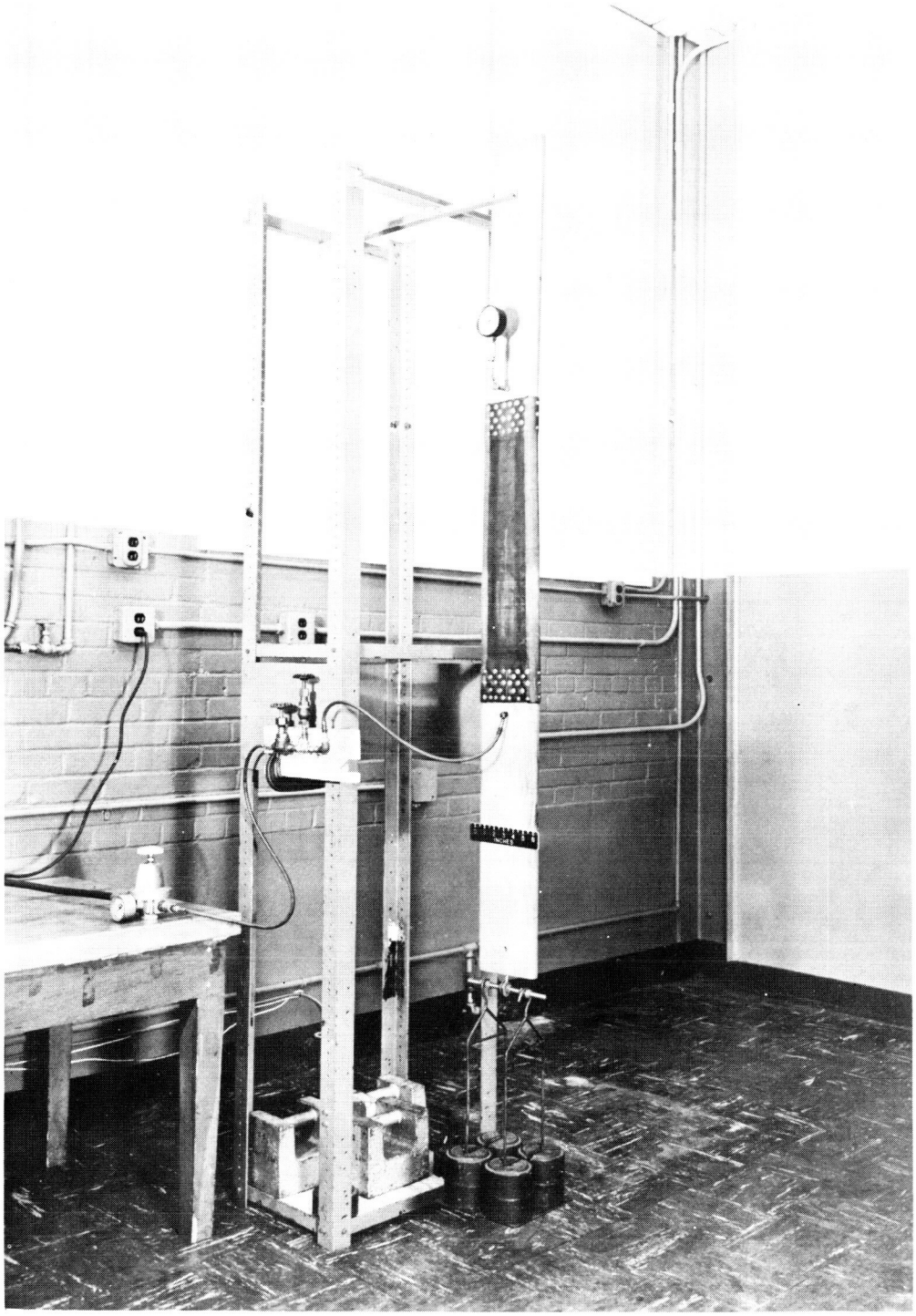

Figure 4.- Beam tension test setup. L-60-4665

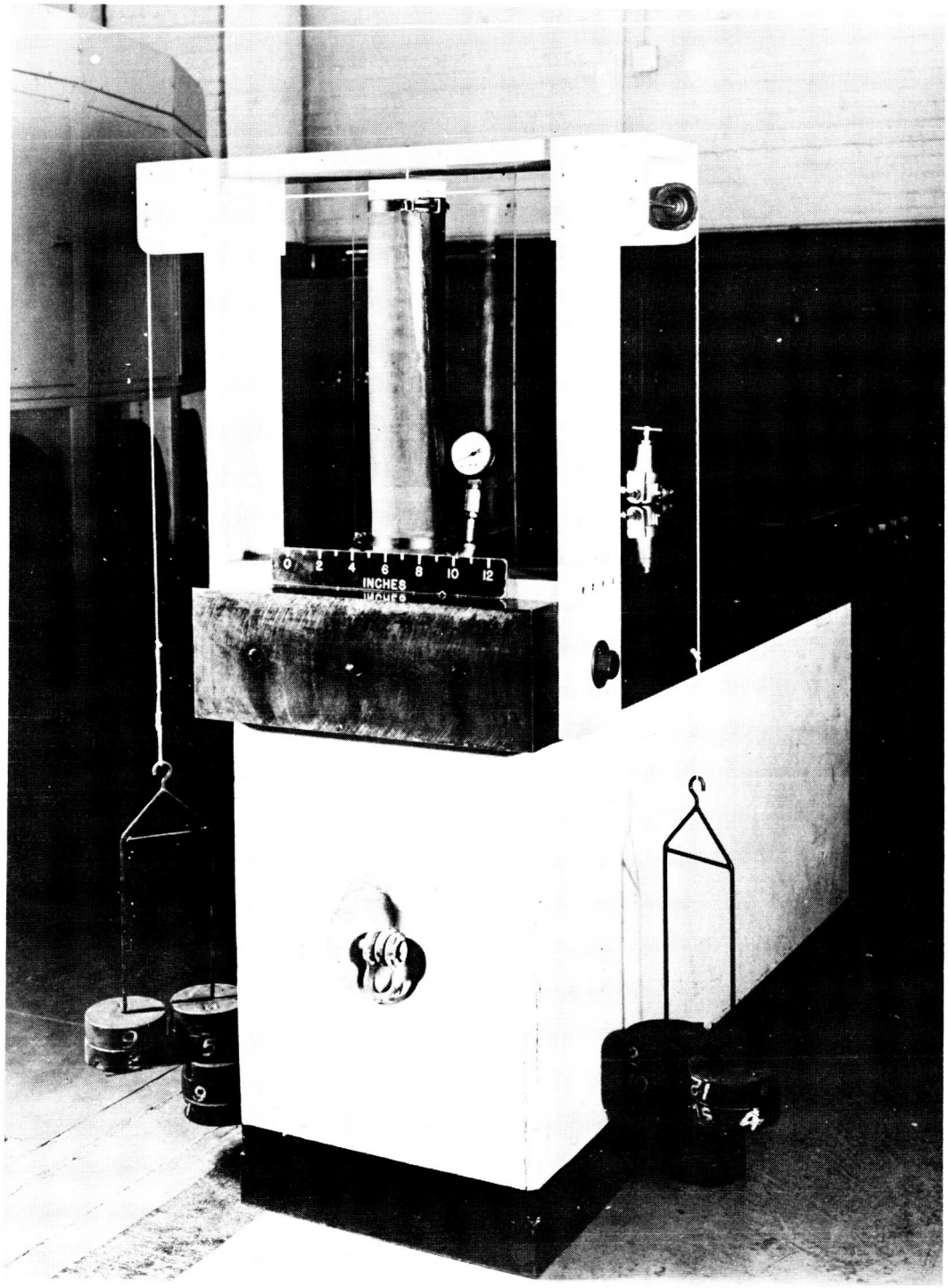

Figure 5.- Cylinder twisting test setup. L-59-5267

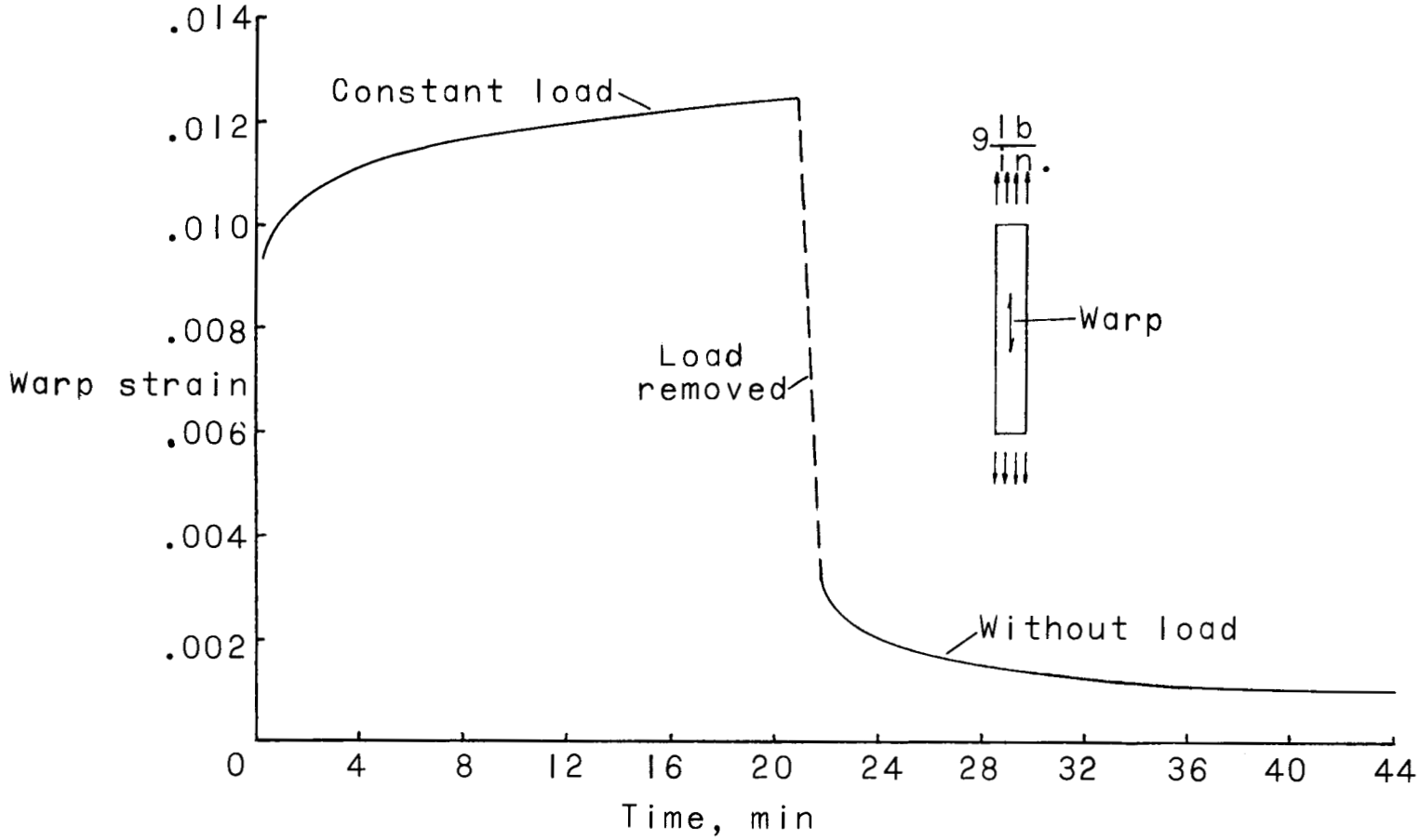

Figure 6.- Effect of time on strain of strip material.

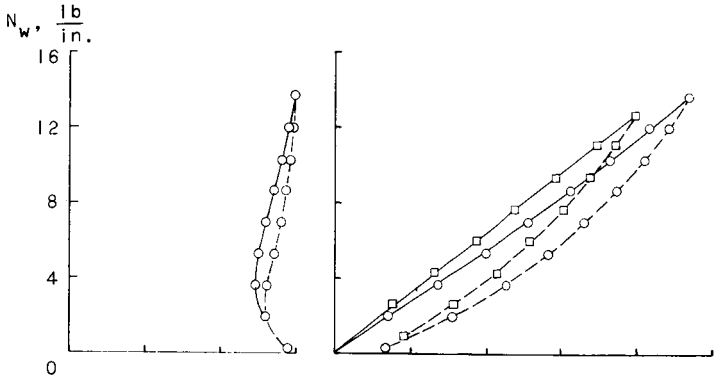

(a) Warp longitudinal.

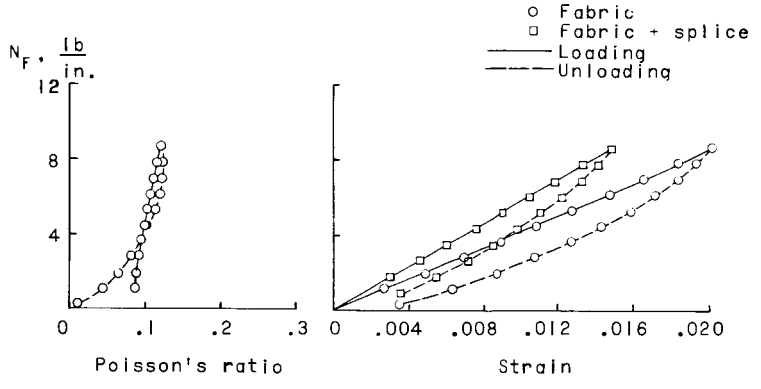

(b) Fill longitudinal.

Figure 7.- Uniaxial stress-strain characteristics and values of Poisson's ratio of strip specimens for low loads.

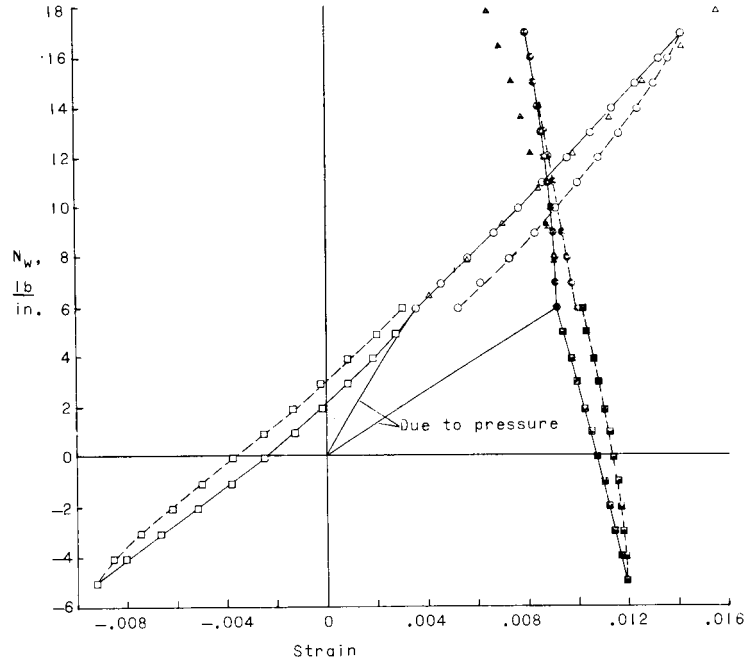

(a) Warp longitudinal.

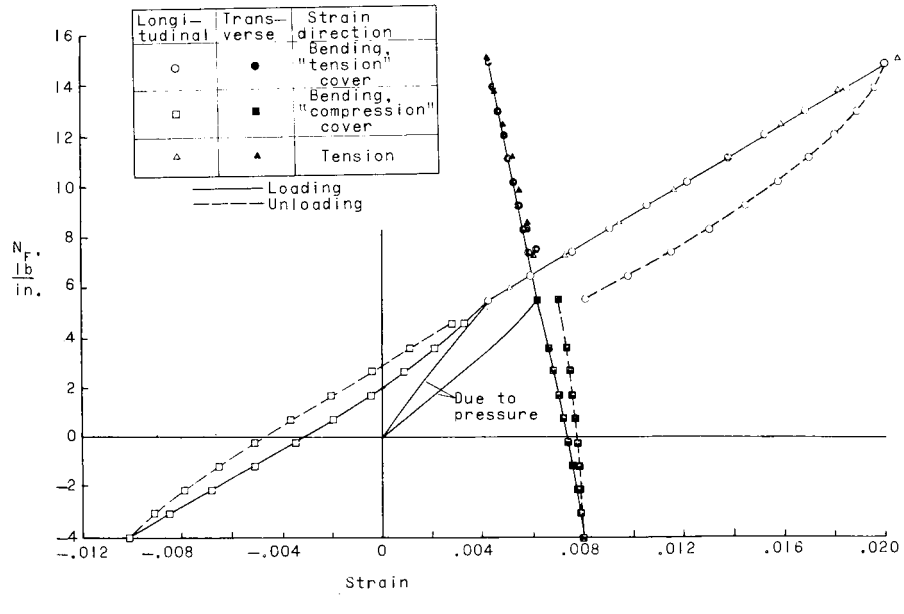

(b) Fill longitudinal.

Figure 8.- Typical stress-strain results for beams with inflation pressure of 15 psig and bending or tension.

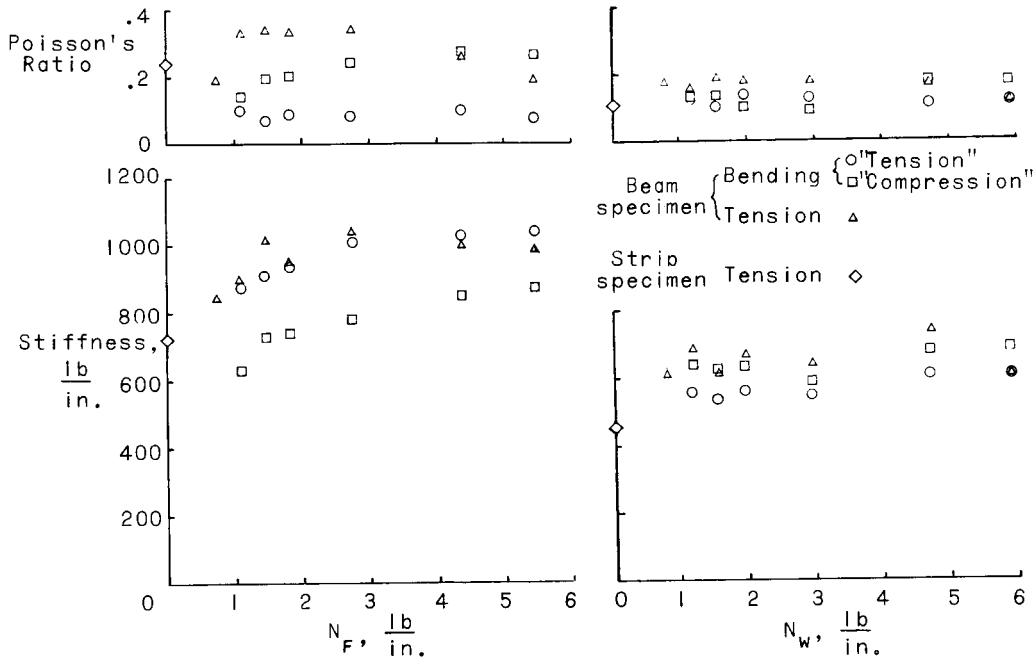

(a) Warp longitudinal. (b) Fill longitudinal.

Figure 9.- Effect of transverse stress due to pressure on stiffness and average values of Poisson's ratio.

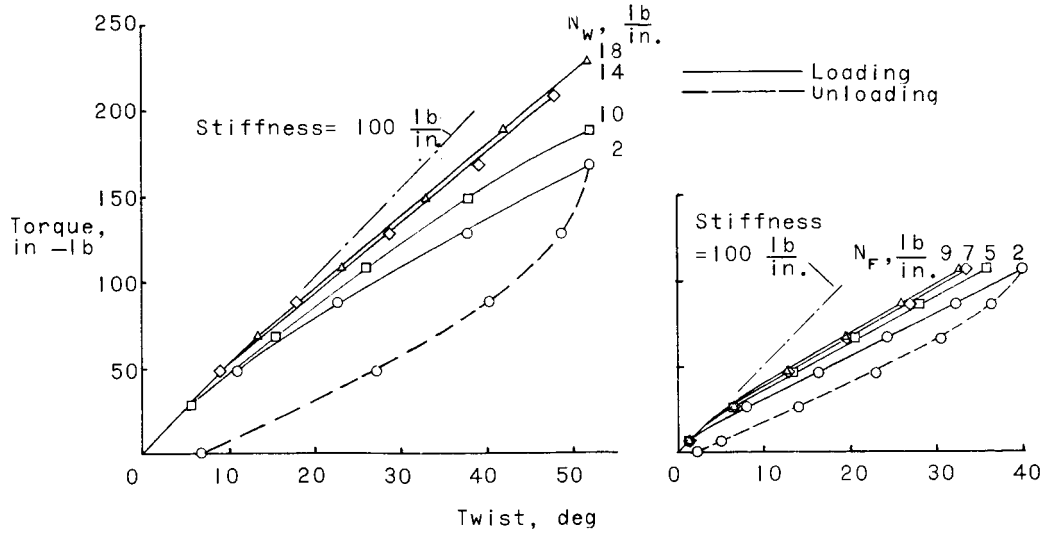

(a) Warp longitudinal. (b) Fill longitudinal.

Figure 10.- Torque plotted against twist for pressurized cylinders.